



The 9th century BCE destruction layer at Tell es-Safi/Gath, Israel: integrating macro- and microarchaeology

Dvory Namdar^{a,b}, Alexander Zukerman^c, Aren M. Maeir^d, Jill Citron Katz^e, Dan Cabanes^{b,g}, Clive Trueman^f, Ruth Shahack-Gross^{b,g}, Steve Weiner^{b,g,*}

^a Institute of Archaeology, Tel Aviv University, Tel Aviv 69978, Israel

^b Kimmel Center for Archaeological Science, Weizmann Institute of Science, Rehovot 76100, Israel

^c F.W. Albright Institute of Archaeological Research, 91100 Jerusalem, Israel

^d Department of Land of Israel Studies and Archaeology, Bar-Ilan University, Ramat-Gan 52900, Israel

^e Department of Sociology, Yeshiva University, New York, NY 10033, USA

^f School of Ocean and Earth Sciences, University of Southampton, Southampton SO17 1BJ, UK

^g Department of Structural Biology, Weizmann Institute of Science, Rehovot 76100, Israel

ARTICLE INFO

Article history:

Received 30 June 2011

Received in revised form

8 August 2011

Accepted 9 August 2011

Keywords:

Microarchaeology

Destruction processes

Phytoliths

Residue analysis

Micromorphology

Fired bricks

ABSTRACT

Destruction events in multi-period sites are valuable marker horizons that represent time-synchronous events across the site and sometimes between sites. Destruction layers often preserve rich finds that provide insights into site use. Here we use both macro- and microarchaeological methods to study a destruction event from the late 9th century at Tell es-Safi/Gath in Israel. A major conflagration at this specific location resulted in the consolidation of parts of the roof construction materials, thus enabling us to differentiate between roof, walls and floor materials. We could reconstruct the events which lead to the formation of an approximately 80 cm thick layer. The base of this layer that overlies the floor surface is a thin charred organic material-rich ash layer. As the clays in this layer were not altered by heat and the ceramics still have preserved residues, we conclude that the ash was produced elsewhere and was redistributed to this location. Ceramics that are associated with burnt roof sediments do not have preserved residues. We also estimate the time that each of the accumulation events might have taken, and conclude that this accumulation occurred over decades. The architecture and artifacts found within and beneath the destruction do not allow us to unequivocally identify the function of this area prior to destruction. We do however identify an unusual bin and associated stone pavement, and a corner rich in artifacts, phytoliths and charred organic material. We also show that a wall was built of fired mud bricks; a most unusual occurrence for this time period in the Levant. This study demonstrates well the usefulness of an integrated macro- and microarchaeological approach to understanding the archaeological record, as well as the benefits of using an on-site laboratory.

© 2011 Elsevier Ltd. All rights reserved.

1. Introduction

The remains of violent destructions are often pivotal points of archaeological stratigraphic sequences in multi-period complex society sites. Destruction layers in the Levant, at least, are up to a meter or so thick and include one architectural phase. The stratum often contains collapsed wall and roof remains, abundant artifacts and a well-defined floor surface, all buried in a generally non-stratified mass of sediment. Destruction layers are thus

thought to represent “time capsules” that preserve assemblages of material culture characteristic of a particular period and region that enable archaeologists to correlate strata within and between sites. In addition, material culture is often well preserved in these contexts, and typically includes abundant finds in primary context, that enable the study of functional aspects of the excavated remains (Hardin, 2011). In the southern Levantine Iron Age, typical examples of such destruction layers are at sites such as Lachish, Beer-Sheba and Tel Halif, destroyed by the Assyrian king Sennacherib in 701 BCE, and the sites of Timnah, Ashkelon and Ekron, destroyed by the Babylonian king Nebuchadnezzar in 604 BCE (Mazar, 1990).

The length of time required for the formation of a destruction layer is not well documented. According to written sources,

* Corresponding author. Department of Structural Biology, Weizmann Institute of Science, Rehovot 76100, Israel.

E-mail address: steve.weiner@weizmann.ac.il (S. Weiner).

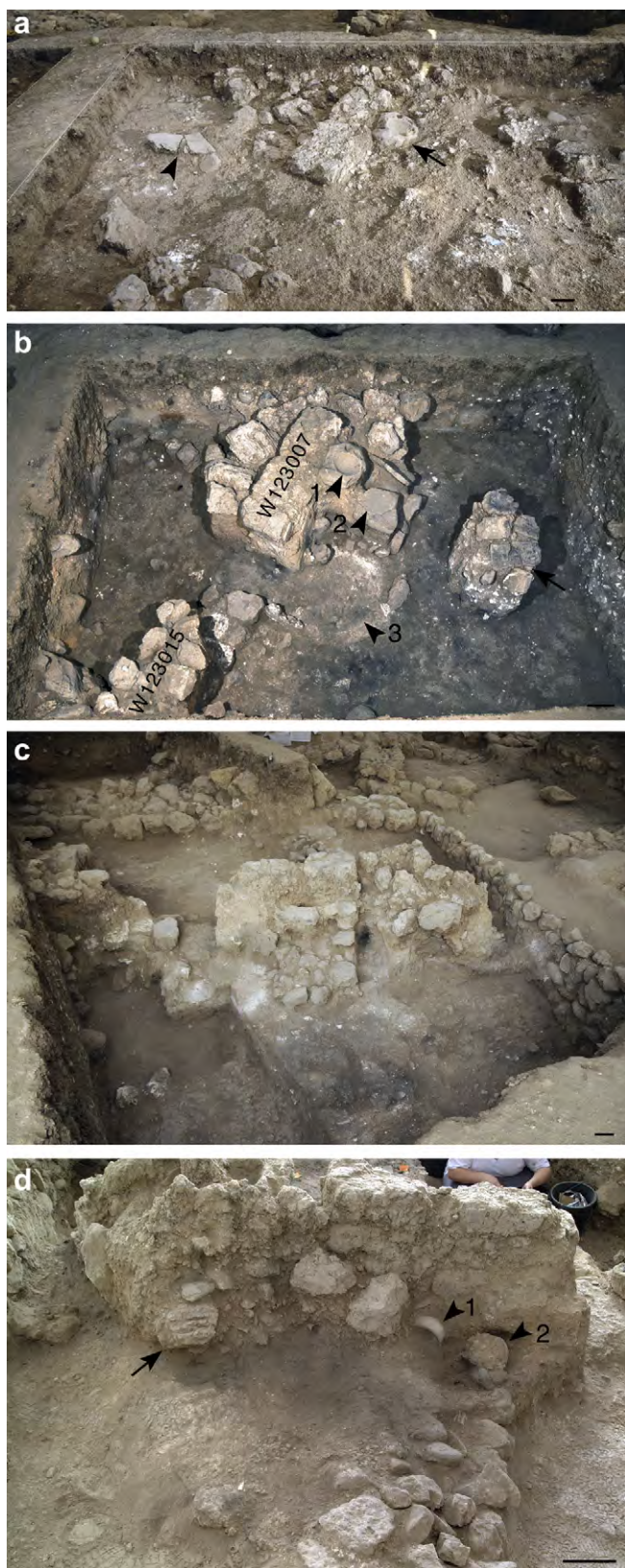


Fig. 3. Photographs of square 89C a. Surface exposed at the beginning of the excavation after the topsoil was removed. The stone mortar and burnt sediment slab are indicated by an arrow and arrowhead respectively. b. Surface exposed after excavation of the ground floor at the end of season 2009. Note the presence of part of the brick wall lying on the sediments in the eastern part of the square (arrow). Also shown (1) stone mortar, (2) grinding stone, and (3) contour of the installation (arrowheads numbered respectively).

excavated, as well as parts of the floor. Samples were analysed on-site and after the season in the laboratory. We note that 500 or more samples were recovered during excavation, and their variable characteristics as determined by infrared spectroscopy, are generally not apparent to the naked eye. This is also the case in many of the baulks.

2.2. Infrared spectroscopy

Infrared spectroscopy was used to identify mineral components, distinguish between carbonates of different origin, and estimate heating temperatures of clay minerals. Infrared spectra were obtained using KBr pellets at 4 cm^{-1} resolution with a Nicolet 200 spectrometer. A rough approximation of relative quartz concentrations was obtained by dividing the height of the main silicate clay peak at around 1035 cm^{-1} by the height of the 797 cm^{-1} peak of the silicate doublet. This doublet is much stronger for quartz than for clay, and hence the ratio of these two peaks reflects relative amounts of quartz (termed the “quartz index”) (Fig. 2a). The relative heights of the calcite ν_2 and ν_4 peaks provide information on the atomic disorder of the calcite (Poduska et al., 2011; Regev et al., 2010). This can be used to distinguish geogenic limestone, from geogenic chalk and plaster. At Tell es-Safi/Gath the degree of crystal disorder in the local chalk is similar to that of calcitic wood ash. The chalk and ash however can often be distinguished by the full width at half maximum height (FWHM) of the ν_3 peak for a specific combination of the normalized ν_2 and ν_4 peaks. Finally an analysis of the clay peaks can distinguish between clays that have been exposed to elevated temperatures and those that have not (Berna et al., 2007). A calibration curve using local clays from Tel es-Safi heated to different temperatures shows that differences can already be discerned in samples heated above $400\text{ }^\circ\text{C}$ (Eliyahu-Behar et al., in press). Note that the peaks that are most sensitive to heat exposure are the small peaks around $3600\text{--}3700\text{ cm}^{-1}$. In many cases it is clear that these peaks are present (designated “not altered” or “na”) (Fig. 2a), or absent (designated “altered” or “a”) (Fig. 2b). In cases where interpretation is equivocal, we place a “?” after the designation.

2.3. Phytoliths

Phytolith concentrations in the sediments were determined during and after the excavation using the method of Katz et al. (2010). Briefly, around 20 mg of homogenized sediment were placed in a 0.5 ml Eppendorf tube and $50\text{ }\mu\text{l}$ of 6 N HCl were added to the sample to dissolve the carbonates. Then $450\text{ }\mu\text{l}$ of sodium polytungstate (2.4 g/l density) were added and the sample was vortexed, sonicated for 20 min and centrifuged at 5000 rpm for 5 min. The supernatant was then transferred to another tube, vortexed and $50\text{ }\mu\text{l}$ of the solution were placed on a slide and covered with cover slip. Phytoliths were counted at 200X and 400X. Phytolith identification was carried out using the standard literature (Mulholland and George Rapp, 1992; Piperno, 1988; Twiss et al., 1969). The International Code for Phytolith Nomenclature was also followed where possible (Madella et al., 2005). The presence of dung spherulites was checked in the laboratory by mounting the original sediment on a slide with Entellan (Merck).

c. Surface exposed at end of season 2010 showing the various walls and roof fall around the brick wall. d. The area to the west of Wall 123007 showing the locations of the burnt sediment with thin branch impressions (arrow), a carrinated bowl (1) and the human skull (2) (arrowhead numbered respectively). Scale bar: 20 cm.

2.4. Organic residues in ceramics

The extraction and analytical procedures for the characterization of lipids associated with ceramics were described elsewhere (Namdar et al., 2010). Briefly, ground pottery was extracted with dichloromethane/methanol (2:1 v/v) by ultrasonication to obtain a total lipid extract (TLE). Prior to analysis, the TLEs were derivatized using *N,O*-bis(trimethyl)silylfluoroacetamide with added 1% (v/v) trimethylchlorosilane, to form trimethylsilyl (TMS) derivatives. The lipid extracts were analysed using a gas chromatograph coupled to a mass spectrometer (GC/MS) (Agilent 7890A GC system and Agilent 5975C VL MSD).

3. Results

The results are divided into two sections: the layer by layer analysis of the destruction horizon, followed by the analysis of the macroscopic and microscopic artifacts that relate to the use of the site at this location.

3.1. Destruction horizon

3.1.1. First indications that excavation square 89C could be of particular interest

A large mortar and a broken flat slab some 20–30 cm long and wide and a few centimeters thick were found immediately below the 20 cm thick topsoil (Fig. 3a). Infrared spectra obtained immediately after exposure of these artifacts showed that the mortar was composed of calcite (indicative of limestone). The slab was actually a mix of approximately equal proportions of clay and calcite, typical of many of the Tel sediments and not of the natural sediments in the area. Furthermore the clay had been altered by exposure to a source of heat that caused the generally loose sediment to consolidate and have ceramic-like properties (Fig. 2b). The tabular nature of this human-made sediment slab, and the fact that the ground storey floor of this structure was well below this level in already excavated adjacent squares, indicated that the slab was probably roof or second storey floor material that had been heated locally (hereafter referred to simply as “roof”, as no clear-cut evidence for the existence of a second storey in any of the Stratum A3 buildings was found so far). We thus chose to examine this location in detail as the consolidation of architectural structures due to exposure to unusually high temperatures, appeared to have preserved some three dimensional structures which could facilitate efforts to identify the architectural origins of the sediments in the destruction horizon. As we knew from excavated

adjacent squares that the ground storey floor of this structure was about 70–80 cm below this level, we sampled the sediments every 10–20 cm as the excavation proceeded. In this way we obtained a 3D overview of the stratigraphic sequence comprising the destruction horizon.

3.1.2. Sequence of layers within the destruction horizon

The more than 500 infrared spectra of the sediments analysed provided the following information for each sample: whether the clays were exposed to temperatures above about 400 °C based on Berna et al. (2007) and Eliyahu-Behar et al. (in press), the relative proportions of quartz and clay and whether the calcite originated from wood ash, plaster or the local geogenic chalk and limestone (Regev et al., 2010) (Fig. 2). In addition we analysed the phytolith concentrations of selected samples from each layer (Katz et al., 2010). We note that mollusk shells found in the sediments were composed of only aragonite (except for those that showed signs of burning). This indicates that the state of mineral preservation is generally very good (Weiner, 2010).

The key to assigning the origin of the non-consolidated sediments is the characteristics of the heat-consolidated materials that still retain their macroscopic shapes. Most of the heat-consolidated materials are located on either side of a brick wall (Wall 123007, see Fig. 3b and c), implying that they had fallen down from the upper part of the wall's superstructure and/or from part of the roof that the wall was supporting. These construction materials include flat slabs ca. 5 cm thick, irregular blocks ca. 10–20 cm in diameter and very large blocks with impressions of aligned thin branches or reeds (Fig. 3d). The consolidated materials have heat altered clay and a quartz index below 10, which indicates a high proportion of quartz. In our assignment of the sources of the unconsolidated sediments listed in Table 1, we therefore ascribe sediments that were heated to above 400 °C and have a high quartz content to roof-related architectural elements (the upper part of roof-supporting walls, the roof itself and the installations located on the roof). The unconsolidated sediments in the eastern part of the area are quite different. These sediments are composed of unburnt or slightly burnt clay, with a low quartz content, and characteristically have angular chunks of chalk of various sizes that were mixed into the sediments (Fig. 4). This “synthetic” sediment type is widely distributed throughout the site in the A3 destruction layer, and in several places drapes over stone wall bases. We therefore assign the functional use of this sediment type to a terre pisé wall construction material (rammed/compressed earth), and infer that there was a terre pisé wall to the east of the examined area. The western wall (Wall 124020) has a very large stone base. We do not

Table 1
Analyses of loose sediment samples from the 7 surfaces analysed in the destruction horizon. The right hand column is our interpretation of the possible source of the sediments from each surface. na - clay not altered by heat exposure; na?-clay probably not altered; a?-clay probably altered; a-clay altered by heat exposure above 400 °C. *Phytolith concentrations from the north–east corner only. Samples were derived from surfaces 5, 6 and 7.

Surface analysed	Depth (meters a.s.l)	Clays (a, a?,na) (:): number of samples	Quartz Index ave ± std	Phytoliths (millions/g) ave ± std	Possible Sediment Source
1	177.15 to 177.04	Na (8), a (7) a? (1)	Mixed 7.8 ± 2.0 n = 8 20.9 ± 3.8 n = 8	1.2 ± 0.3 n = 2	Base of topsoil, top of destruction horizon
2	176.95 to 176.86	a (5),a? (3)	8.9 ± 1.2 n = 8	8.1 ± 1.2 n = 5	Roof
3	176.85 to 176.68	a (8), a? (7), na (4)	19.8 ± 4.2 n = 19	4.6 ± 1.2 n = 10	Mixed
4	176.75 to 176.68	na (11), a (6), a? (1)	8.9 ± 1.7 n = 14	4.5 ± 0.8 n = 4	Roof/walls Terre pisé wall (east)
5	176.69–176.49	a (11), a? (4), na (5)	15.0 ± 3.3 n = 19	6.5 ± 5.2 n = 22 6.2 ± 5.4 (w/o NE corner n = 19)	Roof Terre pisé wall (east)
6	176.51 to 176.36	na (12), na? (2), a (2), a? (1)	17.1 ± 5.3 n = 17	8.7 ± 6.4 n = 24 5.1 ± 2.1 (w/o NE corner n = 16)	Floor upper part
7	176.36–176.22	na (10), na? (2)	11.4 ± 4.0 n = 29	7.9 ± 6.8 n = 16 5.3 ± 3.5 (w/o NE corner n = 11) 13.7 ± 7.0 (NE corner only*)	Floor lower part



Fig. 4. Photograph of the NE corner of the excavation area showing the sediments with blocks of angular chalk, which bury various broken vessels, and the loom weights (not seen). Note too that the chalk-containing sediment surface slopes to the west and the interface with the light brown roof sediment in the lower part of the section is almost vertical. a. Topsoil. b. Roof consolidated (left) and unconsolidated (right) sediment. c. Terre pisé wall. d. Floor upper part. e. Surface of lower part of floor.

know the nature of the construction material above the stone base, although the characteristic angular chunks of chalk seen in the western section of square 89C and in the north–eastern part of adjacent square 88D suggests that its superstructure was also made of terre pisé.

Table 1 (right hand column) shows our assignments of the origins of the sediment layers that comprise the sequence based on the analyses of the sediments from the 7 surfaces that were extensively sampled. Surface 1 is in topsoil. Surface 2 sediments are composed of heat altered sediments, that are quartz-rich and have relatively high phytolith concentrations; all indications of having been derived from the roof. Surface 3 sediments are mixed (heat altered and unaltered sediments) without any indicative characteristics. Surfaces 4 and 5 contained mixed heat altered and unaltered sediments. Most of the latter are from the eastern part of the examined area and are derived from the assumed terre pisé wall beyond the eastern limit of the excavated area. Surfaces 6 and 7 appear to constitute the fine-grained black sediments rich in charred organic material that accumulated on the floor, and the floor itself respectively. Surface 6 contains unaltered clays, and the calcite component is derived from ash based on the grinding curve infrared spectroscopic analysis (Regev et al., 2010). It is therefore surprising that the clay component shows no indications of having been heated above 400 °C. The quartz content is low compared to the clay content. The floor itself is composed of unaltered clay and calcite, and this is underlain by a floor make-up layer that is similar to the floor itself, but more compact. Based on these observations we divide the sediments in the examined area into 5 layers from bottom to top as follows: (1) the constructed floor, (2) the char- and ash-rich sediments on the floor, (3) the roof-derived sediments and/or the terre pisé wall-derived sediments, (4) predominantly roof-derived sediments and (5) topsoil.

Bones in general are not abundant in the examined area. An isolated human skull and several non-articulated human bones were found at one location, under a pile of collapsed building materials just to the west of Wall 123007 (Fig. 3d). These bones appear to belong to a person who died during the initial phase of the destruction, and was subsequently buried under the collapsed

walls. Several additional human skeletons were found on Stratum A3 floors under the destruction debris in an adjacent area of the excavation, outside the presently examined area. A concentration of burnt animal bones was found about a meter away from the human skull and also adjacent to the brick wall 123007 (Fig. 3d). All these human and animal bones were clearly lying in the black fine-grained sediment layer on the floor. For the locations of finds in the examined area, see Figs. 1b and 3.

3.1.3. Variations in phytolith concentrations and assemblages

Table 1 also shows the phytolith concentrations measured in selected samples. The topsoil contains relatively few phytoliths. The layer just below the topsoil (surface 2) contains almost twice as many phytoliths on average than the two surfaces sampled below it. Surfaces 5 to 7 contain higher concentrations than the layers above. However, in these layers there is clearly a high concentration of phytoliths in the NE corner of the examined area (Fig. 4), and if these are removed from the calculation of the average phytolith concentrations, then surfaces 5 to 7 are similar in their low concentrations of phytoliths to surfaces 3 and 4 (Table 1). The distribution of phytoliths thus differentiates surface 2 from the other levels, and shows a high concentration of phytoliths from several levels in the NE corner. This corner also contained several complete ceramic vessels (several storage jars, a cooking jug, a juglet, a large krater, a funnel and other vessels) as well as 21 perforated clay loom weights and a spindle whorl. The sediments were mostly gray in color due to fine-grained charred organic material.

The types of phytoliths in the sediments can be affected by preservation. Cabanes et al. (2011) showed in an *in vitro* experiment that the inflorescence phytoliths of wheat are less stable than the phytoliths of leaves and stems. This can result in better preservation of leaf and stem phytoliths. Cabanes et al. (2011) and Carnelli et al. (2002) also showed that the so-called “weathered” phytoliths are actually present in the plant itself, and that this widely used parameter for assessing preservation may not be reliable. Cabanes et al. (2011) also showed that phytolith morphotypes more prone to dissolution and abrasion are the delicate ones such as

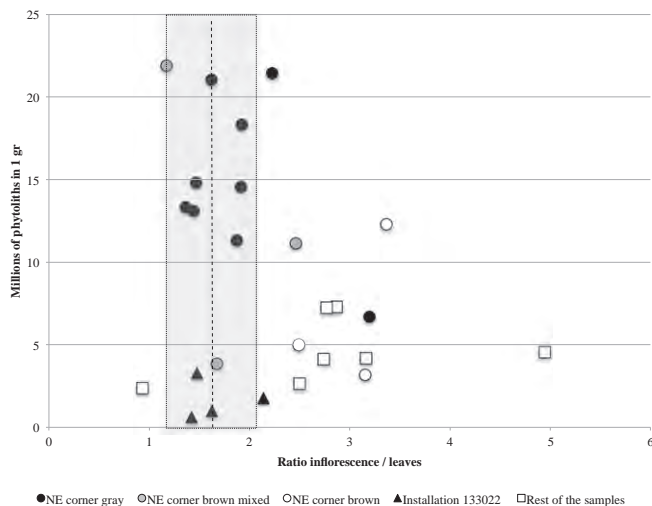


Fig. 5. The number of phytoliths in 1 gr of sediment plotted against the ratio of inflorescence and leaves/stems grass phytoliths.

hairs, papillae and thin decorated long cells. The phytoliths from the whole area under study contained relatively high amounts of the more delicate inflorescence phytoliths of cereals, and the overall proportion of weathered phytoliths was low (Table 1 supplementary material). We therefore conclude that in general the state of phytolith preservation in this area is good.

Most of the phytoliths identified originate from monocotyledonous plants. No characteristic palm phytoliths (spheroid echinates) were detected, and only two indicative phytoliths from *Cyperaceae* were identified. We thus infer that the monocotyledonous phytoliths are from grasses. The identification of short cells indicates that these grasses are mostly from the festucoid subfamily, and the presence of chloridoids and panicoids is minor. The proportion of dicotyledonous phytoliths is also low and is limited mostly to wood and bark phytoliths.

Fig. 5 shows the number of phytoliths in 1 gr of sediment plotted against the ratio of inflorescence to leaves/stems grass phytoliths. The dashed line shows the ratio of one whole *Triticum aestivum* plant from our reference collection, which is 1.6 ± 0.7 . Note that this ratio may differ in other cereals. The gray charcoal-rich samples from the NE corner have a ratio of inflorescence/leaves close to that of the whole plant (with one exception). Samples from other parts of the square, as well as some brown samples from the NE corner have higher proportions of leaves and lower phytolith concentrations.

Cereal inflorescence contains a high amount of dendritic long cells (Rosen, 1992) and a value above 7% has been proposed as being characteristic of cultivated grass (cereal) inflorescence (Albert et al., 2008). Only two samples from the floor level of square 89C yielded

values of dendritic long cells above 7%, whereas echinate long cell morphotypes are more abundant (Table 1 supplementary material). Therefore there is no clear evidence for the presence of cereal inflorescence in the samples analysed, that would indicate grain storage.

The presence of phytoliths from all grass plant parts raises the possibility that the phytoliths were derived mainly from animal dung. Supporting evidence for this possibility, in the form of dung spherulites, was not found.

3.1.4. Ceramic vessels and residue analysis (including adjacent square 88D)

Square 89C yielded several whole or broken ceramic items. While some of the vessels were lying on surfaces 6 and 7 (Fig. 6a), most of the vessels were embedded in the overlying layers above the floor (Fig. 6b). This suggests that the majority of vessels originated from either niches and/or shelves built into the walls (no direct evidence available) or from the roof, which collapsed during or after the initial destruction.

Eleven vessels were analysed for the presence of lipid residues preserved within the ceramic walls. Lipids were only found in the ceramic fragments lying in the black ashy layer of surfaces 6 and 7 ($n = 4$) (Table 2; Fig. 6a). We analysed the sediments in which all 11 vessels were buried. The seven vessels above surfaces 6 and 7 were buried in heat altered clays, whereas the broken pieces lying in the black ashy layer of surfaces 6 and 7 were associated with unaltered clays (Table 2). (For an explanation, see the Discussion, section 4 below). The lipids extracted from the four sherds in layers 6 and 7 (jar 1230115, jar 1230102, krater 1230115 and krater 1230103) indicated that these vessels contained different mixtures of plant oil and animal fat (for example, see Fig. 7a).

The adjacent excavation square (88D) also contained many whole or partially broken vessels associated with the destruction horizon. Here we analysed 13 vessels for their lipid contents and found lipids in 3 vessels that were part of cluster D (Table 2). Here too sediments associated with these lipid-containing vessels showed no indication of having been exposed to elevated temperatures. Most, but not all the sediments associated with the other vessels that did not contain lipids, were exposed to elevated temperatures. These results show that in both these squares one factor that influences lipid preservation in ceramic items is whether or not the vessels or vessel fragments were once exposed to temperatures above 400 °C; the sensitivity threshold for altered clays.

As the infrared spectra of the local clays change structure only above 400 °C or so, we heated fragments of the base of jar 1230115 that contained well preserved lipids (Fig. 7a) for 2 h to 100, 200, 300, 400 and 500 °C. We then analysed the lipids in these fragments and found that after being heated to 100 °C only part of the original lipid assemblage remained in the ceramic matrix. The lipids remaining were mostly fatty acids (Fig. 7b). Heating to 200 °C

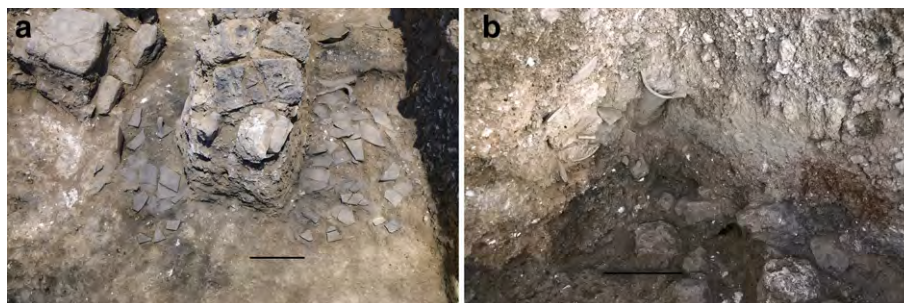


Fig. 6. a. Broken vessels lying on Level 7 floor. b. Broken chalice embedded in the heat altered roof sediments in the NW corner of the area.

Table 2

Lipids extracted from the items included in this study and their association with the sediments around them. na - clay not altered by heat exposure; na?-clay probably not altered; a?-clay probably altered; a-clay altered by heat exposure above 400 °C. (): number of samples.

Locus	Basket	Vessel class	Description	Sampling	Cluster	Organic residues	Associated sediments
Square 88D							
133002	1330020	jar	Store jar with grooved rim	Body	A	–	n.a (3)
133002	1330042	jar	Store jar	Base	A	–	n.a? (1) a? (1) a (2)
133002	1330021	jar	Store jar with short concaved rim	Base	B	–	n.a (1)
133002	1330030	jar	Store jar	Base	B	–	n.a? (2) a (1)
133002	1330004	jar	Store jar	Base	C	–	n.a (3)
133002	1330023	jar	Store jar with black crust on body	Body	C	–	n.a? (3)
133002	1330026	jar	pre- <i>MLK</i> jar	Body	C	–	a? (3) a (1)
133002	1330059	jar	pre- <i>MLK</i> jar	Body	D	++	n.a (11)
133002	1330059	bowl		Base	D	+++	n.a? (3)
133002	1330057	jar	Store jar	Base	D	++	a? (1)
133002	1330057	jar	Store jar	Base	D	–	
133002	1330034	jar	Store jar with short rim	Body	E	–	n.a (6)
133002	1330058	jar	Store jar	Base	E	–	n.a? (4) a (2)
Square 89C							
123012	1230111	bowl	carrinated bowl	Base	1	–	a?
123012	1230111	jar	large metallic jar	Body	1	–	a
123012	1230110	chalice		Joint between body and base	1	–	
123012	1230103	krater		Body	2	–	a (2)
123013	1230102	scoop			3	–	n.a (3)
123013	1230102	jar	Holemouth jar	Rim	3	+	n.a? (1)
123013	1230112	jar	large metallic jar	Body	4	–	a (1)
123013	1230104	jug	Philistine cooking jug	Body	4	–	
123014	1230115	jar		Body	5	+++	n.a (4)
123014	1230115	pitthos		Rim	5	–	
123014	1230115	krater		Body	5	+++	

resulted in all lipids being destroyed (Fig. 7c). This implies that if lipids are preserved, the vessel or vessel fragments were probably not heated to above ca. 100 °C. This is consistent with organic residues being absent in ceramic items associated with heat altered sediments.

3.2. The architectural features

Fig. 3b–d show the main architectural features in the examined area that were exposed after most of the destruction horizon sediments were removed. The center of the area is dominated by a complex of structurally related features: a wall with a narrow 22 cm wide gap (Walls 123007 and 123015), the base of a rounded bin (12022) and associated stone pavements on both sides of Wall 123007 (Pavements 133012 and 133017). Wall 123015 is built of stones to a height of ca. 40 cm above the surface 7 floor and extends for some unknown length into the unexcavated area. Stone wall 133013 abuts Wall 123015 at a right angle, and all three walls (133013, 123015 and 123007) create an L-shaped configuration. See Figs. 1b and 3c for details.

3.2.1. Brick Wall 123007

The brick wall was preserved to a height of about 70 cm above the floor. A collapsed series of bricks was also found in the eastern part of the studied area lying on top of the terre pisé sediments (Fig. 3b). We analysed 3 bricks from this wall, and one brick from a segment of the wall that had fallen to the east and was still partially intact. The brick dimensions are around $15 \times 12 \times 20 \pm 1$ cm. We cut 4 bricks in half and obtained infrared spectra from the center and the periphery. Fig. 8 shows the exposed section of one of the bricks from the collapsed section. The core of this brick still contains charred black organic material. Significantly there is a uniformly thick lighter colored layer on all surfaces that is devoid of black material. Other

sectioned bricks did not have a black core, but infrared analysis showed that they too were uniformly heated from the core to the surface. This uniform heating pattern indicates that the bricks were pre-fired prior to being placed in a wall. The alternative possibility, that a source of heat close to the wall surfaces is responsible for the observed distribution of charred organic material, seems unlikely. All the infrared spectra from the cut exposed surfaces showed the same properties both in the core and close to the 4 surfaces, namely the brick material is composed of an approximately equal mix of calcite and clay, and the quartz content was high (Quartz Index below 10). The clay had clearly been altered by exposure to temperatures around 500–600 °C. All these analyses are consistent with the bricks having been fired prior to use. It should be mentioned that fired bricks are unknown in the Iron Age southern Levant, although they were widely used in Egypt and Mesopotamia from the 3rd millennium BCE onwards (Wright, 2005).

We also analysed the binding material (mortar) between the bricks. This was composed mainly of calcite, and the grinding curve analysis (Regev et al., 2010) showed that the atomic disorder state was between the ash/chalk curves and modern plaster/mortar, indicating that this is indeed a high temperature produced mortar. In contrast to this, all the calcite in the bricks had disorder signatures that were close to the ash/chalk curve, implying that they were more ordered and hence exposed to lower temperatures. We conclude that the mortar used for these walls was indeed a real mortar prepared from slaked lime, and not crushed chalk.

3.2.2. Other Walls

To the north–west is the stone base of a massive wall (Wall 124020). We have no knowledge of the type of sediment that was used for the superstructure above this stone socle, although the characteristic angular chunks of chalk seen in the north–eastern part of adjacent square 88D suggests that it was also made of

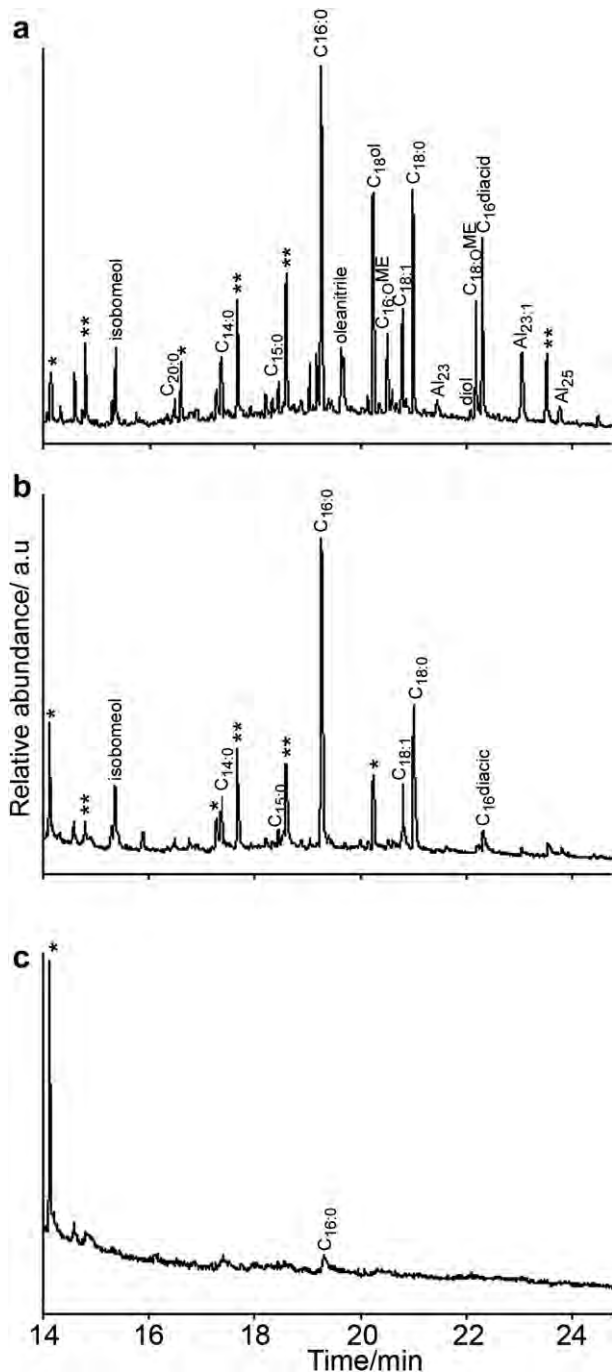


Fig. 7. Lipids extracted from ceramic jar (item 1230115). a. Without any heat treatment, b. After being heated to 100 °C for 2 h, and c. After being heated to 200 °C for 2 h. C/Al_{x:y} – fatty acid/*n*-alkane with *x* carbons in the chain and *y* degree of unsaturation; * - phthalate; ** - silylation by-product.

terre pisé (rammed/compressed earth). As mentioned above, we infer from the talus that entered into square 89C from the SE (Fig. 4), that another wall existed to the south–east, and its superstructure was similarly made of unburnt clay and calcite-rich sediments, together with angular fragments of chalk (i.e., a terre pisé wall). In general, terre pisé is a very common but poorly documented construction material (Braemer, 1982; Wright, 2005).

To the north, the only wall we identified was composed of a one layer thick line of stones (Wall 62021, see Figs. 1b and 3c), which



Fig. 8. Section of one of the bricks from wall 123007 showing that the brick was exposed uniformly to heat on all surfaces.

was not an independent architectural element but rather a revetment. We have not identified a wall to the south, where no excavations to date have been carried out.

3.2.3. Installation 133022

A lower part of a rounded installation (133022) was found abutting the south–eastern face of Wall 123007 (Fig. 3b). The installation (or bin) was at least 50 cm deep based on the curved impression of its outside surface on sediments abutting brick wall (123007). The base of the installation was sunk into the floor and was constructed of a layer of 3–4 cm of almost pure calcite. A grinding curve analysis (Regev et al., 2010) showed that this material was finely ground local chalk and not lime plaster. The chalk layer also contains phytoliths. An analysis of the phytolith morphotypes shows a relatively high proportion of phytoliths from grasses and judging from the presence of dendritic phytoliths, a large proportion of cereals. There is a 22 cm wide gap between Walls 123007 and 123015 that is directly opposite the installation, and may therefore be related to the manner in which it functioned. Two complete vessels, a scoop and a holemouth jar, were found close to the container, on the Levels 6 and 7 floor layers. No lipids were found in the extract of the scoop, while the holemouth jar contained organic biomarkers that point to a plant origin, such as diacids, camphoric acid and borneol (Pavia et al., 1990; Regert et al., 1998).

Samples from the base of the installation have low concentrations of phytoliths from grass leaves, stems and inflorescence. Note too that samples 9729 and 9733, both located near the installation, show respectively the lowest and the highest concentrations of inflorescence among all the samples, even though both of them have relatively low phytolith concentrations (Table 1 supplementary material, Fig. 5). Note also that sample 9729 is the one with a higher percentage of anatomically connected phytoliths (Table 1 supplementary material), implying relatively good preservation (Cabanes et al., 2009; Jenkins, 2009).

The total lipid extract of this chalk (sampled at the bottom of the installation and at a higher point along its profile) showed no detectable lipids, implying that the installation was not used for storing organic liquids, unless the preservation conditions were such that none of the lipids were preserved. We also did not

observe any high concentrations of phosphate in the chalk that could have been derived from organic liquids.

A thin section through the container base (Fig. 9a) confirms that the bulk of the white lining is composed of crushed chalk. Evidence for the chalk being crushed is the presence of a few quartz grains (Fig. 9c, marked by an asterisk) and rounded soil-derived grains (Fig. 9c, marked “s”) that are naturally not present in this rock. In addition, the chalky mass includes planar voids (Fig. 9c, marked “v”) some of which contain grass phytoliths. Such voids are well-known in mud bricks (Friesem et al., 2011) and seem to indicate that the crushed chalk had been tempered with grass material (straw or chaff). This is consistent with the low concentrations of grass phytoliths in the chalk lining. Similar grass-tempered chalk linings have been found attached to walls of the Early Bronze 1B temple in Area J at Megiddo (Friesem and Shahack-Gross, in press).

Immediately above the chalk lining of the installation, a quartz-rich chalky fragment was observed (Fig. 9b). This fragment may have originated from the roof, based on its high quartz content and burned clay component.

3.2.4. Roof

As no part of the roof (or second floor) was preserved intact, we can only deduce aspects of the structure from the collapsed fragments. These fragments included several flat and thin (3–4 cm) slabs of heat-consolidated local sediment (Fig. 3a), including some that still contained the impressions of smoothing by hand. Much larger irregular shaped blocks (up to 50 cm or so in largest dimension) were concentrated in a pile on both sides of brick wall 123007. All these blocks were also consolidated due to exposure to elevated temperatures, and some of them contained well defined

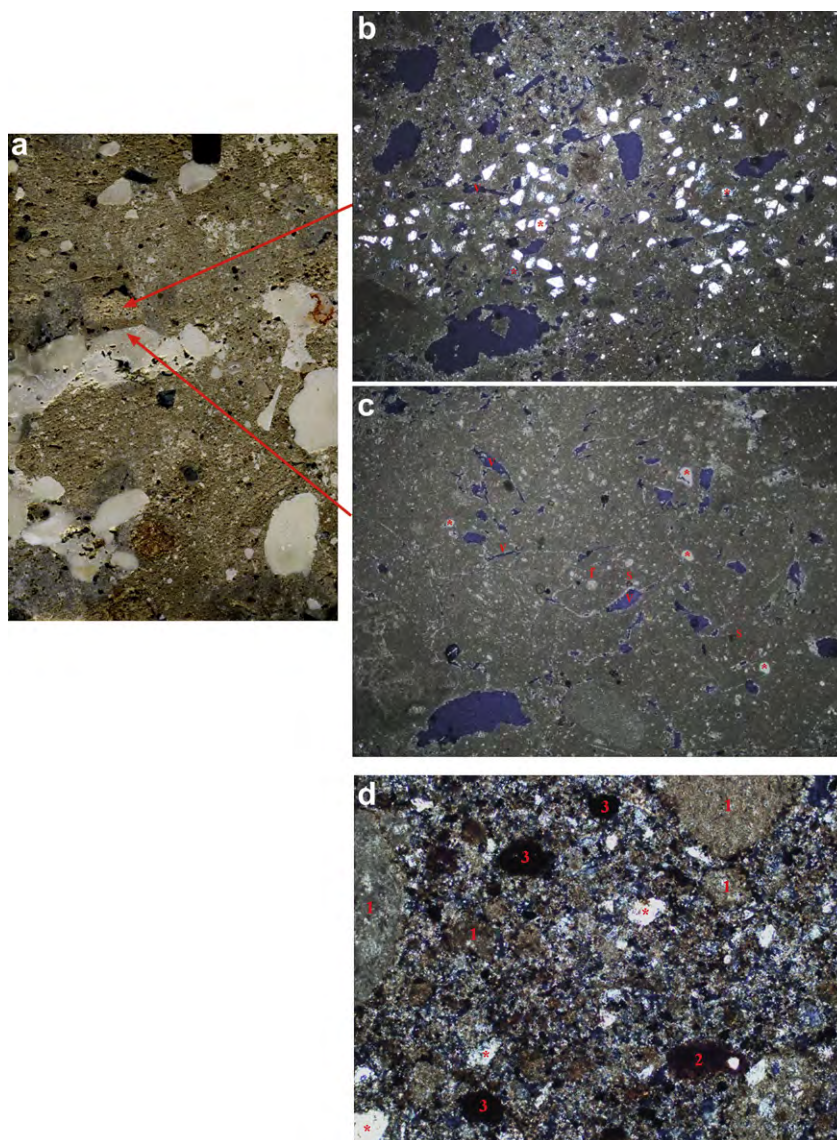


Fig. 9. a. Scan of thin section where the white chalk lining of the installation can be seen (white sub-horizontal layer in middle of slide). Scan width is 4 cm. b. Photomicrograph of the sediment above the chalk lining composed of relatively large amounts of quartz grains (fine sand size) within a chalky mass, possibly representing roof material that collapsed into an empty installation. *: quartz grains, v: void. Field width 7.2 mm. c. Photomicrograph of the installation's chalk lining showing a few quartz grains (*), rounded soil grains (s) and planar voids typical of grass temper (v). Note also the presence of foraminifera microfossils indicative of chalk (f). Field width 7.2 mm. d. Photomicrograph from a thin section containing the charcoal-rich sediment that accumulated on the ground floor level of the destruction horizon in area A. Note the rounded grains of chalk (1), soil-derived material (2) and charcoal (3). Note also the charcoal film around the chalk grains and the absence of groundmass. The grain roundedness, film cover, and lack of groundmass are all indicative of deposition of reworked material. The fine-grained calcite may originate from either poorly preserved wood ash (i.e., no pseudomorphs have been identified in thin section) or from weathered chalk powder. Field width 1.44 mm. All photomicrographs are in crossed polarized light.

impressions of plant stalks on one surface (Fig. 3d). The diameters of these impressions are around 1–2 cm. Judging from the size of the blocks, it is unlikely that such thin branches could support this weight. We also noted that sediment is firmly attached to the one side of the block. We therefore postulate that these blocks were either a continuation of the ground floor brick wall until the roof, or, perhaps, belonged to a parapet on the roof that was supported by the wall.

4. Discussion

Fig. 10 is a schematic reconstruction of the architectural and other features of the excavated area based on the observations above. We have no unequivocal evidence demonstrating the function of the remains uncovered. The partially exposed space was most probably a part of a larger building complex, and the function of the remains analysed here will hopefully be elucidated when placed in a wider spatial context. The functions of the adjacent structures are under study, and their uses ranged from cultic to domestic, industrial and storage (Zukerman and Maier, *in press*). Furthermore, the distribution of the finds may in part reflect the unique moment in time that the building was destroyed, namely at the end of a long siege.

Based on the locations of the non-architectural artifacts, we can distinguish between objects that were located on the roof (as they lie on top of roof debris), objects that were on shelves or niches (associated mainly with wall debris, lying under roof-related debris, but above the floor) or objects that were on the floor or dropped directly onto the floor (located on the floor surface). The stone mortar and large stone grinding tools were located on the roof. The chalice was also probably located on the roof as it was embedded in loose burnt roof sediment. Chalices are known to have been used for burning incense (Namdar et al., 2010), and the location on the roof is in accordance with a well-known Ancient Near Eastern ritual (del Olmo Lete, 2004), connected to events of

stress, such as a siege. The loom weights and other associated vessels from the NE corner were most likely from a niche or shelf as they are buried in terre pisé sediments derived from the inferred wall to the east. The broken vessels in the east of the area, as well as a scoop and holemouth jar, were probably originally on the floor. We note that Iron Age scoops were probably primarily used for redistribution of solid staples (Gitin, 1993). The fact that no lipid remains were detected in the scoop extraction, although found in an unburnt environment (Table 2) may support this notion. Holemouth jars were used for production of oil from olive presses and for short-term storage of liquid and solid commodities. In fact the holemouth jar from square 89C showed the presence of plant oil, following the interpretation of Regert et al. (1998).

Perforated spherical loom weights and a spindle whorl were found in the NE corner of the excavated area, attesting to weaving activity. However, in contrast to more clear-cut archaeological cases (Shamir, 2006), no traces of wooden loom beams were found, and the weights were not found in rows. In fact the weights and other associated vessels had clearly fallen down. Alternatively, these spherical clay objects may be interpreted as (stored) jar stoppers rather than loom weights, as documented, for example, in Iron Age 2A contexts at Tel Zayit, Horbat Rosh Zayit and Tell el-Hammah (Gal and Alexandre, 2000; Homan, 2004).

The evidence for construction techniques and destruction presented in this study, although documented in a limited area, reflects the broader picture observed in other locations in Area A and other excavation areas on Tell es-Safi/Gath where the mid/late 9th century BCE destruction horizon was exposed. For instance, terre pisé used for wall superstructure (on stone foundations) is a common building method in Area D (in the “lower city”), where many such walls were plastered. A high-intensity conflagration that created piles of well consolidated building materials was observed at another location in Area A. That location functioned as a dwelling/storage area, and several brick bins and storage compartments were discovered there.

4.1. The stages of destruction

4.1.1. Stage 1

A major conflagration took place on the ground floor level in the vicinity of this structure, but not within the structure (see below). A particularly intense fire occurred on the roof of the structure. The core of this latter fire was focused in the area immediately above the brick wall, and was hot enough to cause the sediment to fuse and become consolidated. The remaining roof sediments were also exposed to heat above 400 °C, but did not consolidate. Pottery was left intact or smashed and left on the ground floor. A person was killed at this location or close by, and parts of the body were found adjacent to the east side of the brick wall. The duration of the destruction itself was probably hours to days.

4.1.2. Stage 2

A layer of charred organic material-rich ash accumulated on top of the ground floor surface. As the associated clays in this layer were not exposed to heat above 400 °C and lipids were still preserved in the ceramics lying in the char-rich sediment indicating that the temperatures were less than 200 °C, we infer that the fire that produced this char-rich ash was located in the vicinity, but did not burn in the walled area. The fire was presumably part of the destruction process, and following the fire the char-rich ash was redistributed into the ground floor of the walled area, presumably by wind. This black layer is commonly found at other locations on the destruction floor surface. Several thin sections sampled from this black layer across excavation area A show that it is composed of rounded charcoal, soil-derived material (e.g., mud brick or pottery

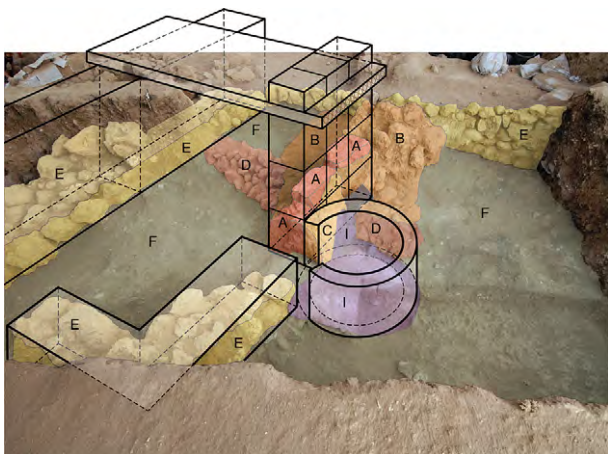


Fig. 10. Schematic drawing overlaid on a photograph of the excavation square at the end of the 2010 season. The colors (and assigned letters) show the extents of the various structural entities (usually loci) and the black lines are the hypothetical reconstructions of the architectural elements. F – the constructed floor and the thin overlying ash layer; E – stone walls; B – roof fall fragments, A – fired brick wall; D – stone pavement on both sides of the fired brick wall; I – installation, and C – imprint of the installation on Wall 123007. Note that we do not know the full extent of the roof, and what is shown is the minimal extent based on the distribution of the consolidated roof fall. The layer of fired bricks overlying the roof was inferred from the presence of the impressions of branches preserved on the surfaces of some of the roof fall blocks. An alternative possibility is that these blocks were derived from the last row of bricks below the roof. (For interpretation of the references to color in this figure legend, the reader is referred to the web version of this article.)

fragments) and chalk grains in a granular microstructure indicative of deposition of reworked materials (Fig. 9d). The grinding curve analysis using the full width at half height of the main calcite peak (see Methods) indicates that much, but not all of the calcite is derived from ash.

We note that the redistributed ash layer is overlain by roof sediments that were exposed to elevated temperatures. This raises the possibility that the fire that produced the floor ash preceded the fire on the roof. The alternative, namely that both fires occurred at the same time, seems less likely as the ash layer and the roof fall would have been mixed.

The fact that only parts of a human body were found raises the possibility that the body was either dismembered during the destruction or scavengers removed parts of the body soon after the destruction. There was no evidence of burial or of the human bones having been burned. Five other partially articulated unburned bodies were found in the nearby cultic context in the same A3 destruction horizon. We also found a group of burned animal bones near the human skull. These burned bones were also lying in sediments that had not been exposed to elevated temperatures. They were presumably burned at some other location either during the destruction or as a result of food preparation. Stage 2 events probably took place during the destruction or within weeks following the destruction.

4.1.3. Stage 3

The ground floor is overlain in certain areas by fine-grained sediments with a burned clay component which we surmise were derived from the parts of the roof that were not subjected to heat that was intense enough to cause consolidation of the sediments. As these sediments overlie the ash layer, the roof must have survived the fire without immediate collapse.

We also observed that sediments from the eastern terre pisé wall directly overlie the ash layer in the eastern part of the area excavated. The fairly smooth surface of these sediments gently slopes to the west and north (Fig. 4), and this slope is reminiscent of a talus that is the product of erosion rather than an irregular pile of sediments that would result from deliberate destruction of a terre pisé wall. In one area the contact between the talus sediments and the burnt roof sediments was seen to be almost vertical (Fig. 4), implying that the accumulations of roof and wall-derived materials occurred more or less simultaneously and hence probably over a fairly long period.

The north–east corner contains a pile of the terre pisé wall sediment with fine-grained charred material, broken ceramic vessels and clay loom weights. This pile lies on the ash layer. As this assemblage is part of the talus (Fig. 4), the artifacts were likely to have been in a niche within this wall, falling down as the wall eroded. The high concentrations of phytoliths and the fine-grained charred material were presumably derived from the vessel contents, bedding or possibly cereal thatch present on the roof. The erosion of the wall could have extended for years or even decades after the destruction.

4.1.4. Stage 4

The upper layers are composed, in part, of the pile of consolidated roof debris that is concentrated around the brick wall. Within this pile are several large and heavy grinding stones and on the very top of the pile was a massive stone mortar. We therefore infer that this part of the roof remained standing for a long period of time after the destruction, probably because the intense fire had consolidated the sediments. Furthermore, because the wall was composed initially of fired bricks, it was relatively sturdy compared to terre pisé or sun-dried mud bricks. In fact some of the bricks fell onto the terre pisé sediments after they had been eroded from the

wall. In the areas further away from the brick wall more burned roof sediment accumulated, together in places with unburnt sediment. This wall and the associated roof probably stood for decades following the initial conflagration.

The results of this study, as well as similar evidence from other parts of the excavation of this destruction level, indicate that the process of destruction that resulted in an 80 cm or so thick accumulation of sediments and artifacts was not a single, rapid event. Rather it appears that there are several stages in the processes related to the formation of the destruction horizon. The destruction itself was not a uniform process, but rather, different parts of the architectural features and the associated material culture followed different destruction pathways. Some were burnt, some collapsed, some eroded and others remained standing for an extended period. Skeletal evidence indicates that casualties of this destruction were left in the open, some partially covered, some completely uncovered. Only at a later stage were the skeletal remains covered by sediments. We therefore conclude that the destruction horizon may have taken tens of years to accumulate.

4.2. Broader archaeological implications

The site of Gath of the Philistines was destroyed by Hazael of Aram Damascus in ca. 830 BCE. Following this destruction, Gath is no longer considered a major polity in the southern Levant (Maier, 2004, *in press*). The apparent abandonment of the site (as indicated by the lack of burial of the victims of the destruction, the absence of looting of intact vessels and the fact that the destruction sequence remained undisturbed during its accumulation) is supported by the archaeological evidence at Tell es-Safi/Gath that the site was not resettled in any substantial manner until about a century later, probably in the late 8th cent. BCE, when the site was temporarily annexed by the Judahite kingdom. In addition, evidence from other portions of the site appears to indicate that during the mid-8th cent. BCE, the site was struck by an earthquake, and collapsed walls, seemingly due to a major seismic event, were found (Maier, *in press*). Thus the “complex” process of destruction as revealed by macro- and microarchaeological methods fits in well with relevant historical evidence (Chadwick and Maier, *in press*; Maier, *in press*).

4.3. The macro- and microarchaeological approaches

Here we show that an integrated study of a confined area within a large site can produce more information than separate studies of the macroscopic remains and aspects of the analyses of various materials. This study also demonstrates the importance of having some on-site analytical capability. Without this, the potential of this excavation area would probably only have been recognized until after most of the area had been excavated, with a resultant loss of much of the information. By focusing this intensive work on a limited area, we did not impede the overall progress of the excavation.

This study has some direct implications for the analysis of lipids in ceramics (“residue analysis”). We showed that lipids are absent in sediments whose clay component had been heated to above 200 °C. This is probably the main reason why most, but not all the ceramics in the destruction horizon do not contain lipids. It is thus imperative to characterize the microenvironments around such ceramics in order to avoid sampling ceramics that are not likely to have any preserved lipids, and/or to better understand the reason for the absence of lipids. Heat exposed clays are often abundant in sites that we have analysed in the Levant (Berna et al., 2007; Elyahu-Behar et al., *in press*).

5. Conclusions

Here we show that: (1) the 80 cm or so thick destruction horizon from the mid/late 9th century BCE was formed by a variety of processes that could have extended for decades, during which time the site remained abandoned, resulting in an accumulation of sediments; (2) Different parts of even this small area underwent different degradation and accumulation processes; (3) We differentiated between artifacts that were originally located on the roof, in niches or on shelves, and on the ground floor; (4) We identified fired bricks from a period in which this practice was unknown; (5) We demonstrate that the absence of lipids in many of the ceramics is probably due to heat exposure, and that residue analysis research should include a study of the microenvironment in which the ceramics are buried.

Acknowledgments

We thank Prof Israel Finkelstein for his helpful comments. This study was under the auspices of the European Research Council under the European Community's Seventh Framework Programme (FP7/2007–2013)/ERC grant agreement n° 229418. It was also supported in part by the Kimmel Center for Archaeological Science, Weizmann Institute of Science, and by a grant (to A. Maeir) from the Israel Science Foundation (grant number 324/10). D.C. has a post-doctoral fellowship from the Beatrice de Pinós program (Departament d'Universitats, Recerca i Societat de la Informació de la Generalitat de Catalunya).

Appendix. Supplementary material

Supplementary data related to this article can be found online at doi:10.1016/j.jas.2011.08.009

References

- Albert, R.M., Shahack-Gross, R., Cabanes, D., Gilboa, A., Portillo, M., Sharon, I., Boaretto, E., Weiner, S., 2008. Phytolith-rich layers from the Late Bronze and Iron Ages at Tel Dor (Israel): mode of formation and archaeological significance. *Journal of Archaeological Science* 35, 57–75.
- Berna, F., Behar, A., Shahack-Gross, R., Berg, J., Boaretto, E., Gilboa, A., Sharon, I., Shalev, S., Shilstein, S., Yahalom-Mack, N., Zorn, J.R., Weiner, S., 2007. Sediments exposed to high temperatures: reconstructing pyrotechnological processes in Late Bronze and Iron Age strata at Tel Dor (Israel). *Journal of Archaeological Science* 34, 358–373.
- Braemer, F. (1982). *L'architecture domestique du Levant à l'Age du Fer*. Paris.
- Cabanes, D., Burjachs, F., Expósito, I., Rodríguez, A., Allué, E., Euba, I., Vergés, J.M., 2009. Formation processes through archaeobotanical remains: the case of the Bronze Age levels in El Mirador cave, Sierra de Atapuerca, Spain. *Quaternary International* 193.
- Cabanes, D., Weiner, S., Shahack-Gross, R., 2011. Stability of phytoliths in the archaeological record: a dissolution study of modern and fossil phytoliths. *Journal of Archaeological Science* 38, 2480–2490.
- Carnelli, A.L., Madella, M., Theurillat, J.P., Ammann, B., 2002. Aluminum in the opal silica reticule of phytoliths: a new tool in palaeoecological studies. *American Journal of Botany* 89, 346–351.
- Chadwick, J.R., Maeir, A.M. How households can illuminate the historical record: the Judahite houses at Gath of the Philistines (a case study in household archaeology at Tell es-Safi/Gath, Israel), in: Foster, B.P.A.C. (Ed.), *Household Archaeology: New Perspectives from the Near East and Beyond*, Winona Lake, IN, in press.
- del Olmo Lete, G. (2004). *Canaanite religion according to the liturgical texts of Ugarit*. Winona Lake, IN.
- Eliyahu-Behar, A., Yahalom-Mack, N., Shilstein, S., Zukerman, A., Shafer-Elliott, C., Maeir, A.M., Finkelstein, I., Weiner, S. Iron and bronze production in Iron Age IIA Philistia: new evidence from Tell es-Safi/Gath, Israel. *Journal of Archaeological Science*, in press.
- Eph'al, I., 2009. *The City Besieged: Siege and its Manifestations in the Ancient Near East*. Culture and History of the Ancient Near East Brill, Leiden.
- Friesem, D., Boaretto, E., Eliyahu-Behar, A., Shahack-Gross, R., 2011. Degradation of mud brick houses in an arid environment: a geoarchaeological model. *Journal of Archaeological Science* 38, 1135–1147.
- Friesem, D., Shahack-Gross, R. Area J. Part V: Analyses of sediments from the level J-4 Temple floor. in: Finkelstein, I., Ussishkin, D., Cline, E. (Eds.), *Megiddo V: The 2004–2008 Seasons*, Monograph Series of the Institute of Archaeology, Tel Aviv University, Tel Aviv. in press.
- Gal, Z., Alexandre, Y., 2000. *Horbat Rosh Zayit. An Iron Age Storage Fort and Village*. Israel Antiquities Authority Reports, Israel Antiquities Authority, Jerusalem.
- Gitin, S., 1993. Scoops: corpus, function and typology. In: Heltzer, M., Segal, A., Kaufman, D. (Eds.), *Studies in the Archaeology and History of Ancient Israel in Honor of Moshe Dothan*, pp. 99–126. Haifa.
- Hardin, J.W., 2011. Understanding houses, households, and Levantine archaeological record. In: Yasur-Landau, A., Ebeling, J.R., Mazow, L.R. (Eds.), *Household Archaeology in Ancient Israel and Beyond*. Brill, Leiden, Boston, pp. 9–25.
- Homan, M.M., 2004. Beer and its drinkers: an ancient Near East love story. *Near Eastern Archaeology* 67, 84–95.
- Jenkins, E., 2009. Phytolith taphonomy: a comparison of dry ashing and acid extraction on the breakdown of conjoined phytoliths formed in *Triticum durum*. *Journal of Archaeological Science* 36, 2402–2407.
- Katz, O., Cabanes, D., Weiner, S., Maeir, A.M., Boaretto, E., Shahack-Gross, R., 2010. Rapid phytolith extraction for analysis of phytolith concentrations and assemblages during an excavation: an application at Tell es-Safi/Gath, Israel. *Journal of Archaeological Science* 37, 1557–1563.
- Madella, M., Alexandre, A., Ball, T., Grp, I.W., 2005. International code for phytolith nomenclature 1.0. *Annals of Botany* 96, 253–260.
- Maeir, A.M., 2004. The historical background and dating of Amos VI 2: an archaeological perspective from Tell es-Safi/Gath. *Vetus Testamentum* 54, 319–334.
- Maeir, A.M., 2008. Tel Zafit. In: Stern, E. (Ed.), *New Encyclopedia of Archaeological Excavations in the Holy Land*. Jerusalem, pp. 2079–2081.
- Maeir, A.M., 2009. Hazael, Birhadad, and the hrz. In: Schloen, D. (Ed.), *Exploring the Longue Durée: Essays in Honor of Lawrence E. Stager*, pp. 273–277. Winona Lake, IN.
- Maeir, A.M. Philistia and the Judean Shephelah after Hazael: the power play between the Philistines, Judeans and Assyrians in the 8th century BCE in light of the excavations at Tell es-Safi/Gath, in: Berlejung, A. (Ed.), *Disaster and Relief Management in Ancient Israel, Egypt and the Ancient Near East*, Tübingen. in press.
- Maher, E.F., 2006, 2007. Imminent invasion: the abandonment of Philistine Ekron. *Scripta Mediterranea* 27–28, 323–337.
- Mazar, A., 1990. *Archaeology of the Land of the Bible 10,000–586 B.C.E.* Doubleday, New York.
- Mulholland, S.C., George Rapp, J., 1992. Phytolith systematics: an introduction. In: George Rapp, J., Mulholland, S.C. (Eds.), *Phytolith Systematics: Emerging Issues*. Plenum Press, New York - London, pp. 1–13.
- Namdar, D., Neumann, R., Weiner, S., 2010. Residue analysis of chalices from the repository pit. In: Kletter, R., Ziffer, I., Zwickel, W. (Eds.), *Yavneh I - The excavation of the 'Temple Hill' Repository Pit and the Cult Stands*, 30. Friborg, pp. 167–173. OBO Series Archaeologica.
- Pavia, D.L., Lampman, G.M., Kriz, G.S., Engel, R.G., 1990. *Introduction to Organic Laboratory Techniques: A Microscale Approach*. Harcourt Brace College Publishers, New York.
- Piperno, D.R., 1988. *Phytolith Analysis: an Archeological and Geological Perspective*. Academic Press, San Diego.
- Poduska, K.M., Regev, L., Boaretto, E., Addadi, L., Weiner, S., Kronik, L., Curtarolo, S., 2011. Decoupling local disorder and optical effects in infrared spectra: differentiating between calcites with different origins. *Advanced Materials* 23, 550–554.
- Regert, M., Bland, H.A., Dudd, S.N., Van Bergen, P.F., Evershed, R.P., 1998. Free and bound fatty acid oxidation products in archaeological ceramic vessels. *Proceedings of the Royal Society of London B* 265, 2027–2032.
- Regev, L., Zukerman, A., Hitchcock, L., Maeir, A.M., Weiner, S., Boaretto, E., 2010. Iron age hydraulic plaster from Tell es-Safi/Gath, Israel. *Journal of Archaeological Science* 37, 3000–3009.
- Rosen, A.M., 1992. Preliminary identification of silica skeletons from Near Eastern archaeological sites: an anatomical approach. In: Rapp, G., Mulholland, S.C. (Eds.), *Phytolith Systematics Emerging Issues*. Plenum Press, New York, pp. 129–148.
- Shamir, O., 2006. The assemblage of clay loomweights from stratum P-7 building 28636. In: Mazar, A. (Ed.), *Excavations at Tel Beth-Shean 1989–1996, Vol. 1, From the Late Bronze Age IIB to the Medieval Period*. Jerusalem, pp. 478–482.
- Twiss, P.C., Suess, E., Smith, R.M., 1969. Morphological classification of grass phytoliths. *Soil Science Society of America* 33, 109–115.
- Weiner, S., 2010. *Microarchaeology. Beyond the Visible Archaeological Record*. Cambridge University Press, Cambridge, New York.
- Wright, G.R.H., 2005. Materials, technology and change in history. In: *Ancient Building Technology, Vol. 2*. Leiden.
- Zuckerman, S., 2007. Anatomy of a destruction: crisis architecture, termination rituals and the fall of Canaanite Hazor. *Journal of Mediterranean Archaeology* 20, 3–32.
- Zukerman, A., Maeir, A.M. The Stratigraphy and Architecture of Area A, in: Maeir, A.M. (Ed.), *Excavations at Tell es-Safi/Gath*. Wiesbaden. in press.